

# Lawrence Berkeley National Laboratory

## Lawrence Berkeley National Laboratory

### Title

Photoluminescence of Energetic Particle-Irradiated  $\text{In}_x\text{Ga}_{1-x}\text{N}$  Alloys

### Permalink

<https://escholarship.org/uc/item/2w40s4xz>

### Authors

Li, S.X.  
Jones, R.E.  
Haller, E.E.  
[et al.](#)

### Publication Date

2005-12-14

Peer reviewed

## Photoluminescence of Energetic Particle-Irradiated $\text{In}_x\text{Ga}_{1-x}\text{N}$ Alloys

S. X. Li, R. E. Jones, and E. E. Haller,

Materials Sciences Division, Lawrence Berkeley National Laboratory, and Department of  
Materials Science and Engineering, University of California, Berkeley, California 94720

K. M. Yu, W. Walukiewicz, J. W. Ager III, and Z. Liliental-Weber

Materials Sciences Division, Lawrence Berkeley National Laboratory, Berkeley,  
California 94720

Hai Lu and William J. Schaff

Department of Electrical and Computer Engineering, Cornell University, Ithaca, New  
York 14853

### **Abstract:**

A study of the photoluminescence (PL) characteristics of  $\text{In}_x\text{Ga}_{1-x}\text{N}$  alloys in which the Fermi level is controlled by energetic particle irradiation is reported. In In-rich  $\text{In}_x\text{Ga}_{1-x}\text{N}$  the intensity of the PL emission initially increases with irradiation dose before falling rapidly at high doses. This unusual trend is attributed to the location of the average energy of the dangling-bond type native defects (the Fermi level stabilization energy, or  $E_{\text{FS}}$ ), which lies about 0.9 eV above the conduction band edge of InN. As a result of this atypically high position of  $E_{\text{FS}}$ , irradiation-induced defects formed at low doses are donors, and do not act as efficient recombination centers. Thus, low dose irradiation increases the electron concentration and leads to an increase of the photoluminescence intensity. However, at higher irradiation doses, the Fermi level approaches  $E_{\text{FS}}$ , and the defects formed become increasingly effective as a non-radiative recombination centers and the PL quenches quickly. Our calculations of the PL intensity based on the effect of the electron concentration and the minority carrier lifetime, show good agreement with the experimental data. Finally, the blue shift of PL signal with increasing electron concentration is explained by the breakdown of momentum conservation due to the irradiation damage.

PACS numbers: 78.66.Fd, 78.40.Fy

Electronic Mail: w\_walukiewicz@lbl.gov

The discovery of the narrow bandgap of InN at  $\sim 0.7$  eV [1,2] opened up many new applications for the nitrides. For example, it has been recognized that the bandgap range of the  $\text{In}_x\text{Ga}_{1-x}\text{N}$  alloy system (0.7-3.4 eV) is an almost perfect match for the solar spectrum, which makes it a potential material for tandem solar cells [3]. Previous studies have demonstrated that  $\text{In}_x\text{Ga}_{1-x}\text{N}$  alloys exhibit superior radiation resistance of electronic and optical properties over other materials commonly used in tandem solar cells [3,4]. The superior radiation hardness is attributed to the energy position of the irradiation-induced native point defects, which is high above the bandgap [4]. In this paper, we show an unusual dependence of the photoluminescence characteristics of  $\text{In}_x\text{Ga}_{1-x}\text{N}$  on the location of the Fermi energy relative to the average energy of the native defects (the Fermi level stabilization energy).

Epitaxial InN and  $\text{In}_x\text{Ga}_{1-x}\text{N}$  thin films (310-2700 nm thick) were grown on c-sapphire substrates by molecular beam epitaxy (MBE) with a GaN buffer layer [5]. The initial free electron concentrations in these samples ranged from the low  $10^{18}$  to low  $10^{17}$   $\text{cm}^{-3}$  and the mobility ranged from 20 ( $x = 0.37$ ) to above 1500  $\text{cm}^2/\text{V}\cdot\text{s}$  ( $x = 1$ ). An n-type GaN sample with an initial electron concentration of  $7.74 \times 10^{17}$   $\text{cm}^{-3}$  and a mobility of 189  $\text{cm}^2/\text{V}\cdot\text{s}$  was also used in this study. For comparison, we have also studied an n-type GaAs sample and an n-type  $\text{Ga}_{0.5}\text{In}_{0.5}\text{P}$  sample.

The samples were irradiated with 1 MeV electrons ( $5 \times 10^{15}$ - $1 \times 10^{17}$   $\text{cm}^{-2}$ ), 2 MeV protons ( $2 \times 10^{13}$ - $2 \times 10^{15}$   $\text{cm}^{-2}$ ), and 2 MeV  $^4\text{He}^+$  particles ( $2 \times 10^{13}$ - $1.8 \times 10^{16}$   $\text{cm}^{-2}$ ). In all cases, the particle penetration depth greatly exceeded the film thickness, assuring a homogeneous damage distribution along the depth of the samples. Ion channeling spectroscopy showed that the InN film remained single crystalline after the highest dose

of  $^4\text{He}^+$  irradiation. Cross-sectional transmission electron microscopy of the same sample showed that no additional extended defects were formed, indicating that point defects are responsible for the observed changes in properties of the irradiated samples. To scale the irradiation damage of different particles the displacement damage dose methodology is applied [6,7]. The displacement damage dose ( $D_d$ ) is defined as the product of the non-ionizing energy loss (NIEL) and the particle fluence. In this report, the NIEL values were obtained from either Ref. [6] or the SRIM (the Stopping and Range of Ion in Matters) program. The samples were characterized by photoluminescence (PL) spectroscopy. The PL signals were generated by excitation with the 325 nm line of a HeCd laser or the 515 nm line of an argon laser, and were measured by a photomultiplier tube, a Ge photodiode, or an InSb detector, as appropriate.

Figure 1 shows the evolution of the PL spectra of InN and  $\text{In}_{0.32}\text{Ga}_{0.68}\text{N}$  with increasing doses of  $^4\text{He}^+$  irradiation. In both samples the PL signals broaden and their peak positions shift to higher energy as the irradiation dose increases. In the irradiated InN sample (2.7 $\mu\text{m}$  thick), Fabry-Perot oscillations with a period of  $\sim 0.06$  eV modulates the PL spectrum. In both samples the PL intensity first increases at low doses ( $D_d < 5 \times 10^{14}$  MeV/g) and then decreases at higher doses. In the case of  $\text{In}_{0.32}\text{Ga}_{0.68}\text{N}$ , the PL intensity increases by a factor of 2.5 after a dose of  $2.9 \times 10^{14}$  MeV/g. Fig. 2 summaries the irradiation dose-dependence of the relative PL intensities, normalized to the corresponding as-grown samples, for  $\text{In}_x\text{Ga}_{1-x}\text{N}$  alloys over the entire composition range. For comparison, the relative PL intensity of GaAs and  $\text{Ga}_{0.5}\text{In}_{0.5}\text{P}$ , which are materials in current tandem solar cells, are also shown. The results in Fig. 2 indicate a superior radiation resistance of  $\text{In}_x\text{Ga}_{1-x}\text{N}$  compared to standard tandem solar cell materials. For

example, the PL intensity of Ga<sub>0.5</sub>In<sub>0.5</sub>P and GaAs decreased rapidly to 0.4% and 1.1% of the original intensity, respectively, at  $D_d \sim 10^{12}$  MeV/g. The PL intensity of GaN, on the other hand, decreased to 14% of the original intensity at  $D_d \sim 2 \times 10^{13}$  MeV/g. In striking contrast, the PL intensity of InN and In<sub>x</sub>Ga<sub>1-x</sub>N alloys increased slightly with irradiation dose, and did not decrease significantly until  $D_d > 10^{15}$  MeV/g.

The unusual PL behavior is closely related to the effects of irradiation-induced native point defects in In<sub>x</sub>Ga<sub>1-x</sub>N alloys. According to the amphoteric defect model, the properties of dangling-bond-type native point defects are determined by the location of the Fermi energy ( $E_F$ ) relative to the Fermi level stabilization energy ( $E_{FS}$ ), an average energy for dangling bond-type defects in all semiconductors [8,9]. As shown in Fig. 3,  $E_{FS}$  is located  $\sim 4.9$ eV below the vacuum level, and falls inside the band gap for GaAs, Ga<sub>0.51</sub>In<sub>0.49</sub>P and In<sub>x</sub>Ga<sub>1-x</sub>N alloys with  $x < 0.34$  [4]. It rises into the conduction band for In<sub>x</sub>Ga<sub>1-x</sub>N alloys with  $x > 0.34$  and is located 0.9 eV above the conduction band edge in InN. The character (donor or acceptor) of native defects produced by the irradiation depends on the position of  $E_F$  relative to  $E_{FS}$ . For  $E_F < E_{FS}$  ( $E_F > E_{FS}$ ), donor-like (acceptor-like) defects are primarily produced by the irradiation, moving  $E_F$  toward  $E_{FS}$ . Consequently, as is evident from Fig. 3, donors are expected to be the dominant radiation-induced defects in In-rich In<sub>x</sub>Ga<sub>1-x</sub>N alloys. Incorporation of these donor defects increases the electron concentration and raises  $E_F$ . At sufficiently high irradiation doses, acceptor and donor defects are generated at similar rates, stabilizing  $E_F$  at  $E_{FS}$ . Under these conditions, the electron concentration saturates and the sample becomes insensitive to further irradiation damage. In contrast,  $E_{FS}$  is located inside the bandgap of GaAs,

$\text{Ga}_{0.5}\text{In}_{0.5}\text{P}$ , and Ga-rich  $\text{In}_x\text{Ga}_{1-x}\text{N}$  ( $x < 0.34$ ). If these materials are initially n-type, irradiation will produce acceptor-like defects that compensate the n-type activity [4].

It is well recognized that defect levels near mid-gap are the most effective non-radiative recombination centers, because they have a high probability of capturing both electrons and holes [10-12]. Therefore, the rapid irradiation-induced quenching of the PL intensity in GaAs,  $\text{Ga}_{0.5}\text{In}_{0.5}\text{P}$ , and Ga-rich  $\text{In}_x\text{Ga}_{1-x}\text{N}$  can be attributed to the nonradiative recombination centers formed inside the bandgap by irradiation damage. On the other hand, in In-rich  $\text{In}_x\text{Ga}_{1-x}\text{N}$ , the irradiation-induced defect levels are located above the CBE, forming an energy barrier for trapping of electrons and preventing the defect centers from acting as non-radiative recombination centers. At lower irradiation doses the non-radiative recombination rate does not change significantly due to this barrier. The PL intensity increases due to the increasing concentration of the majority carriers (electrons). However, at higher electron concentration,  $E_F$  approaches  $E_{FS}$  and the barrier for electron trapping is reduced. The irradiation-induced native defects become more effective non-radiative recombination centers, quenching the PL intensity. In Fig. 4, the relative PL intensity of an InN sample is plotted as a function of  $E_F$  (derived from the carrier concentration obtained from Hall effect measurements). As expected, the PL intensity increases slightly for the lower values of  $E_F$  (0.7 – 0.9 eV), and then drastically diminishes when  $E_F > 0.9$  eV.

The broadening and blue shift of PL signal at higher irradiation doses, as shown in Fig 1, can be attributed to the increase of electron concentration and the breakdown of the k-selection rule in heavily-damaged material. A numerical analysis of the effect of n-type doping on the shape and energy position of the PL in InN can be found in Ref. [13].

The shift of the PL emission peak has been sometimes confused with the shift of the fundamental absorption edge or the so-called Burstein-Moss shift [14,15]. In fact, the shift of the absorption edge associated with radiative transitions to the empty states above the Fermi energy in the conduction band [16] is much larger than the shift of the PL emission associated with transitions from the occupied states below the Fermi energy. This is clearly illustrated in Fig. 1, where the overlap of the Fabry-Perot oscillations and the PL signal of irradiated InN indicates that the Burstein-Moss shift of the absorption edge makes the sample transparent in the spectral range of the PL emission.

The relative PL intensity of  $\text{In}_x\text{Ga}_{1-x}\text{N}$  reflects the minority carrier (hole) lifetime in the samples. We can assume that the PL intensity  $I$  is proportional to both the carrier concentration  $N_e$  and the minority carrier lifetime  $\tau$ :

$$I(E_F) \propto N_e(E_F)\tau(E_F) \quad (1)$$

The minority carrier lifetime, affected by both radiative and non-radiative recombination, can be expressed by the following equation:

$$1/\tau = 1/\tau_0 + N_t\sigma v/[1 + \exp(E_{FS} - E_F)/kT] \quad (2)$$

where  $\tau$  is the minority carrier lifetime of the irradiated samples,  $\tau_0$  is the lifetime of the unirradiated samples (radiative recombination lifetime,  $\sim 10^{-9}$  s [17]),  $N_t$  is the concentration of irradiation-induced non-radiative recombination traps (proportional to the increase in carrier concentration),  $\sigma$  is the capture cross-section area of the irradiation-induced defects ( $\sim 10^{-12}$  cm<sup>2</sup> [18]), and  $v$  is the velocity of the minority carriers (holes). To qualitatively account for the broadening effects due to the inhomogeneity of the samples and the breakdown of k-selection rule we have broadened the Fermi energy dependent PL intensity with a Gaussian function characterized by the broadening parameter  $\Delta$ .

Previously, we have used the same broadening procedure to explain the shape of the absorption edges in  $\text{In}_x\text{Ga}_{1-x}\text{N}$  [16]. The calculated PL intensity is plotted in Fig. 4. The calculation shows good agreement with experimental results. The best fit was obtained for  $\Delta = 0.20$  eV which is consistent with the broadening parameter used to describe the shape of the fundamental absorption edge in irradiated InN [16].

In conclusion, it is found that the PL intensity increases at low doses of irradiation due to an increase of the electron concentration. At high doses, when the Fermi level approaches the Fermi level stabilization energy, the native defects become efficient nonradiative recombination centers and quench the PL intensity.

We thank L. Reichertz for providing the GaAs sample. This work is supported by the Director, Office of Science, Office of Basic Energy Sciences, Division of Materials Sciences and Engineering, of the U.S. Department of Energy under Contract No. DE-AC03-76SF00098. The work at Cornell University is supported by ONR under contract NO. N000149910936. One of us (REJ) thanks the U.S. Department of Defense for support in the form of a National Defense Science and Engineering Graduate fellowship.



## References:

- [1] V. Yu. Davydov, A. A. Klochikhin, R. P. Seisyan, V. V. Emtsev, S. V. Ivanov, F. Bechstedt, J. Furthmueller, H. Harima, A. V. Mudryi, J. Aderhold, O. Semchinova, and J. Graul, *Phys. Stat. Sol. B* **229**, R1 (2002).
- [2] J. Wu, W. Walukiewicz, K.M. Yu, J.W. Ager III, E.E. Haller, H. Lu, W.J. Schaff, Y. Saito, Y. Nanishi, *Appl. Phys. Lett.* **80**, 3967 (2002).
- [3] J. Wu, W. Walukiewicz, K. M. Yu, W. Shan, and J. W. Ager III, E. E. Haller, Hai Lu and William J. Schaff, W. K. Metzger, and Sarah Kurtz, *J. Appl. Phys.* **94**, 6477 (2003) and references therein.
- [4] S. X. Li, K. M. Yu, J. Wu, R. E. Jones, W. Walukiewicz, J. W. Ager III, W. Shan, E. E. Haller, Hai Lu, and William J. Schaff, *Phys. Rev. B*, **71**, 161201(R) (2005).
- [5] H. Lu, William J. Schaff, Jeonghyun Hwang, Hong Wu, Goutam Koley, and Lester E. Eastman, *Appl. Phys. Lett.* **79**, 1489 (2001).
- [6] S. R. Messenger, G. P. Summers, E. A. Burke, R. J. Walters, and M. A. Xapsos, *Progress in Photovoltaics: Research and Applications*. **9**, 103 (2001).
- [7] S. R. Messenger, E. A. Burke, G. P. Summers, M. A. Sapsos, R. J. Walters, E. M. Jackson, and B. D. Weaver, *IEEE Trans. Nuclear Sci.* **46**, 1595 (1999).
- [8] W. Walukiewicz, *Appl. Phys. Lett.* **54**, 2094 (1989).
- [19] W. Walukiewicz, *Physica B*, **302**, 123 (2001).
- [10] J. M. Langer and W. Walukiewicz, *Mater. Sci. Forum* **196–201**, 1389 (1995).
- [11] D. D. Nolte, *Solid-State Electron.* **33**, 295 (1990).
- [12] D. E. Aspnes, *Surf. Sci.* **132**, 406 (1983).
- [13] B. Arnaudov, T. Paskova, P.P. Paskov, B. Magnusson, E. Valcheva, B. Monemar, H. Lu, W.J. Schaff, H. Amano, and I. Akasaki, *Superlattices and Microstructures* **36**, 563 (2004).
- [14] K.S.A. Butcher, T.L. Tansley, *Superlattices and Microstructures* **38**, 1 (2005)
- [15] J. C. Ho, P. Specht, Q. Yang, X. Xu, D. Hao, and E. R. Weber, *J. Appl. Phys.* **98**, 093712 (2005).
- [16] S. X. Li, E.E. Haller, K. M. Yu, W. Walukiewicz, J. W. Ager III, J. Wu, W. Shan, Hai Lu, and William J. Schaff, *Appl. Phys. Lett.* **87**, 161905 (2005).
- [17] Fei Chen, A. Cartwright, S. X. Li, K. M. Yu, R. E. Jones, W. Walukiewicz, unpublished.

[18] X. G. Guo, W. Lu, X. S. Chen, and J. C. Cao, *Semicond. Sci. Tech.* **19** 1325 (2004).

Figure Captions:

Figure 1: Room-temperature PL spectra of as-grown and  $^4\text{He}^+$ -irradiated InN and  $\text{In}_{0.68}\text{Ga}_{0.32}\text{N}$ . The corresponding displacement damage doses ( $D_d$ ) are also shown. In the irradiated InN sample (2.7 $\mu\text{m}$  thick), Fabry-Perot oscillations with a period of  $\sim 0.06$  eV modulates the PL signals. Note that in the InN spectra the features at  $\sim 0.75$ - $0.95$  eV are due to water absorption.

Figure 2: Summary of the effect of energetic particle irradiation on the normalized PL intensity of  $\text{In}_x\text{Ga}_{1-x}\text{N}$ , GaAs, and  $\text{Ga}_{0.51}\text{In}_{0.49}\text{P}$ . For reference the  $D_d$  ranges of 1 MeV electrons, 2 MeV protons, and 2 MeV  $^4\text{He}^+$  are labeled.

Figure 3: Band offsets of  $\text{In}_x\text{Ga}_{1-x}\text{N}$  alloys [Wu1], GaAs, and  $\text{Ga}_{0.5}\text{In}_{0.5}\text{P}$  and the Fermi stabilization energy ( $E_{\text{FS}}$ ).

Figure 4: The relative PL intensity of InN from experiments (circles) and from calculations (line).

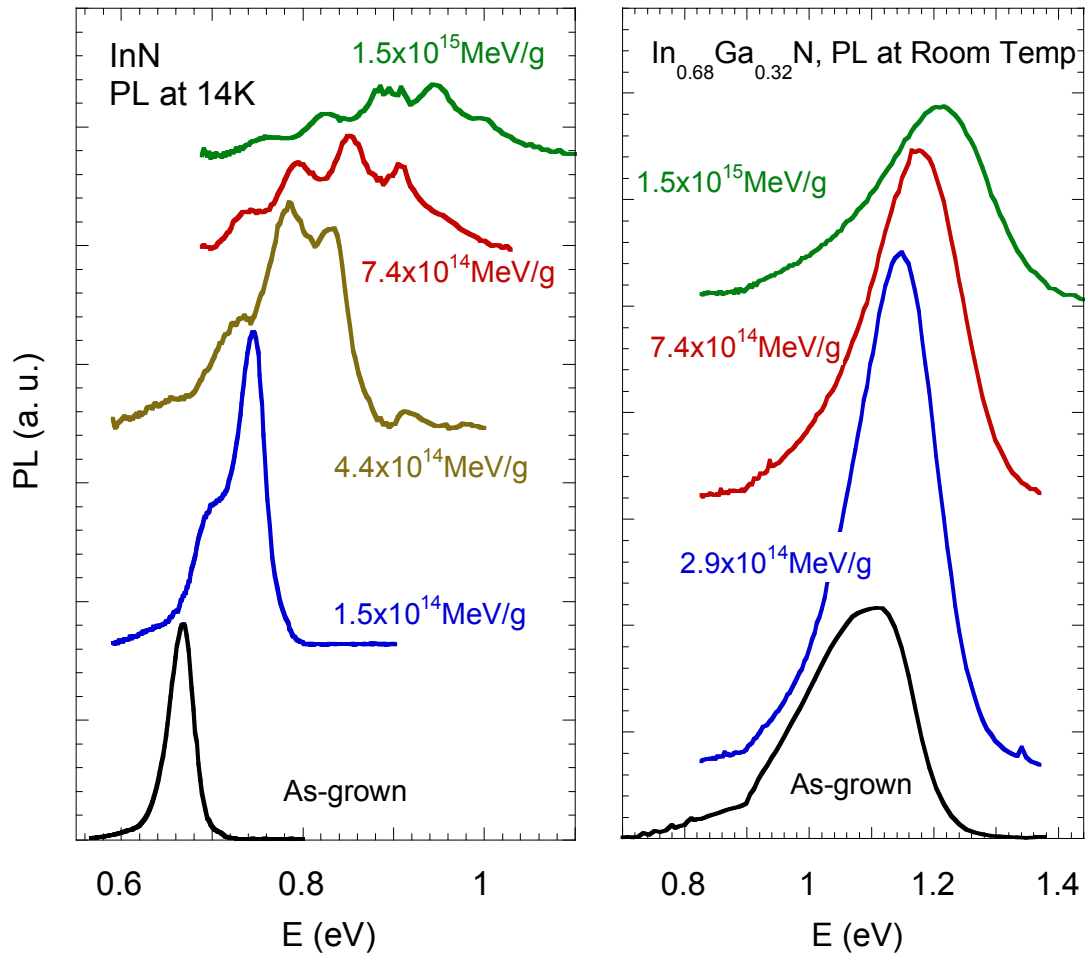


Fig. 1 of 4  
 Li *et al.*

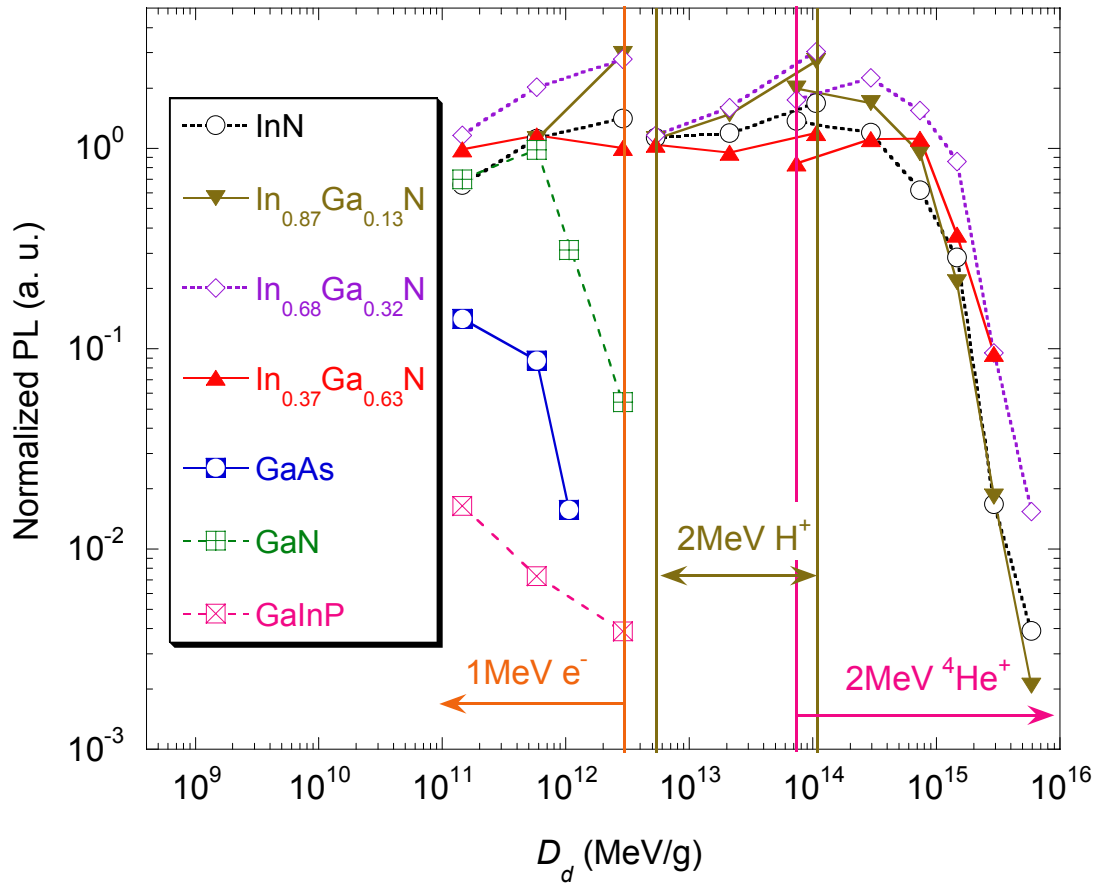


Fig. 2 of 4

Li *et al.*

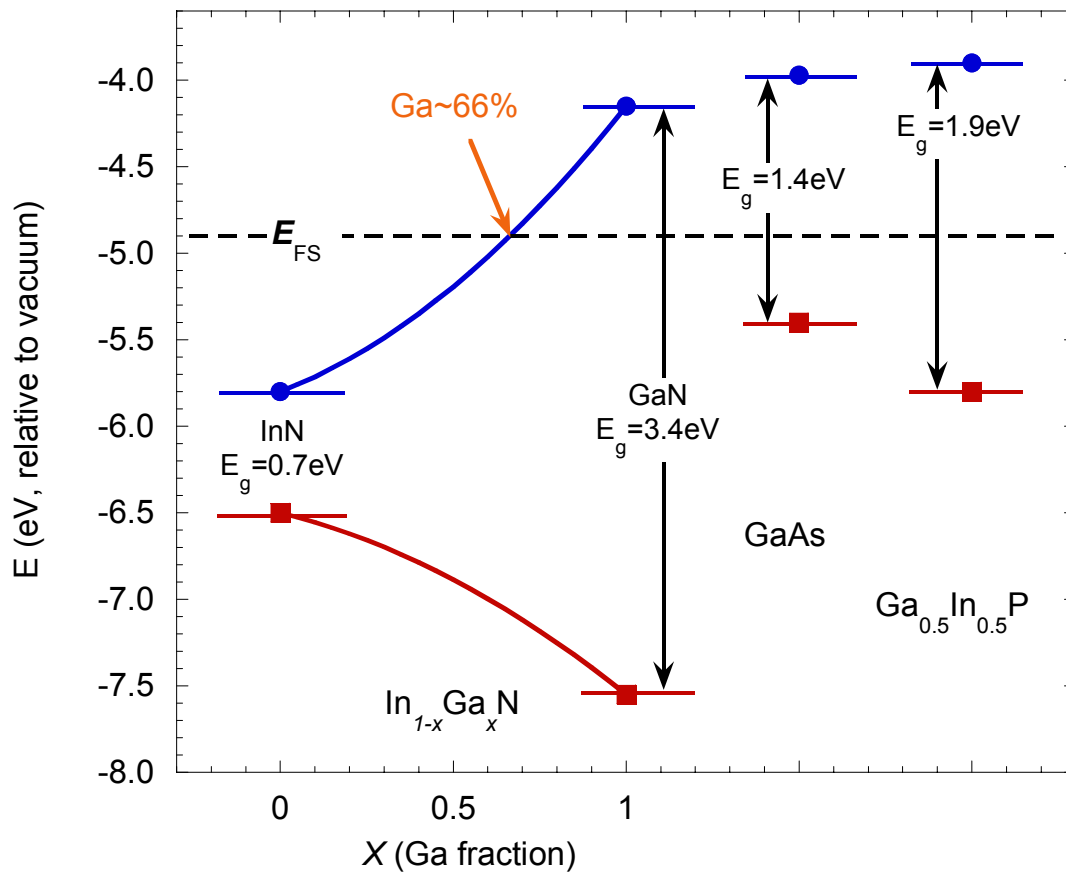


Fig. 3 of 4

Li *et al.*

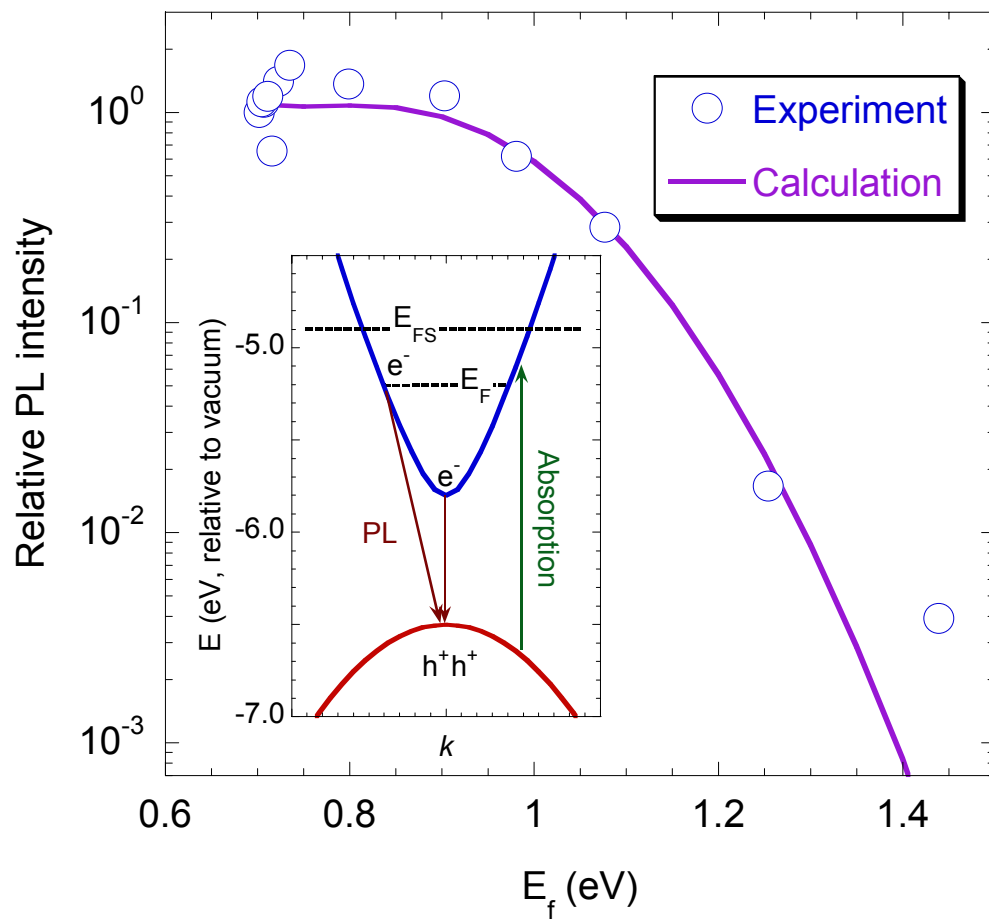


Fig. 4 of 4  
Li *et al.*